Proceedings of the 11th ICPMG 2026
11th International Conference on Physical Modelling in Geotechnics
8-12 June 2026, Zurich, Switzerland

Centrifuge model test of GRS walls under pseudostatic seismic loading

B.V.S. Viswanadham
Professor, Department of Civil Engineering, Indian Institute of Technology Bombay, Mumbai, India
viswam@civil.iitb.ac.in

S. Mukherjee*
Assistant Professor, Department of Civil Engineering, Indian Institute of Technology Madras, Chennai, India
*sougatamukh94@gmail.com, (*Formerly, Institute Post Doctoral Fellow, Department of Civil Engineering, Indian Institute of Technology Bombay, Mumbai, India)*

ABSTRACT: The seismic stability of geosynthetic-reinforced soil (GRS) walls is conventionally evaluated by estimating the dynamic active thrust exerted on the wall under a specified seismic acceleration. However, this approach does not capture wall deformations, which are a critical serviceability criterion for GRS walls. This study investigates the pseudostatic seismic response of GRS walls through centrifuge model testing. Wall-facing deformations and reinforcement strains were quantified using digital image analysis (DIA), while displacement contours within the backfill were derived from particle image velocimetry (PIV) analysis. The pseudostatic seismic loading was applied by rotating the GRS wall model on a tilt-table simulator at 40 g in a large beam centrifuge facility available at IIT Bombay. Results show that wall-facing displacements increase with increasing seismic load intensity. Under static conditions, the maximum wall deformation was approximately 2.4%, which increased sharply beyond an acceleration of 0.1g, exceeding the allowable wall movement of 4% at an acceleration of 0.16g. A similar amplification of reinforcement strains was observed at higher seismic intensities. The PIV analysis revealed a bilinear active failure wedge inclined at approximately 26°, which is significantly lower than the inclination angle predicted by the Mononobe-Okabe (MO) limit-equilibrium method.

1 INTRODUCTION

The stability of geosynthetic-reinforced soil (GRS) walls has been studied extensively over the last few decades. Researchers have employed several methodologies, including laboratory experiments, field studies, numerical modelling, probabilistic analysis, and centrifuge modelling, to assess the GRS wall stability under different conditions.

Besides the major studies focused on the static stability of the GRS wall, the response of GRS wall under seismic conditions has also received ample attention in the literature. For instance, Bathurst and Cai (1995) provided the stability of GRS walls with modular block facings under pseudostatic conditions using the Mononobe-Okabe theory. El-Emam and Bathurst (2007) and Latha and Santhakumar (2015) reported results from shake-table analyses of GRS walls with rigid facings through 1g small-scale physical model tests. However, all these studies have analysed seismic wall behaviour through small-scale laboratory experiments, which do not accurately represent the actual field stress conditions. The actual stresses and deformations within a field-scale GRS wall can be simulated in a centrifuge model by applying high gravity conditions to a carefully constructed small-scale physical model. The current study presents the pseudostatic seismic response of a 10 m high GRS wall (prototype dimensions) through centrifuge experiments (at 40g). Advanced image processing techniques, such as digital image analysis (DIA) and particle image velocimetry (PIV), have been employed to extract wall, reinforcement, and soil displacement results.

The following sections present the scaling laws utilised in the centrifuge experiments and the pseudostatic simulator setup, followed by the physical GRS model tested in the centrifuge and the results obtained from the pseudostatic analysis.

2 SCALING LAWS FOR GRS WALLS IN CENTRIFUGE

The linear dimensions in the centrifuge model such as the height of the GRS wall (H), reinforcement length (L_R), reinforcement vertical spacing (S_v) were scaled down by a factor of N, i.e., $\frac{H_p}{H_m} = \frac{L_{Rp}}{L_{Rm}} = \frac{S_{vp}}{S_{vm}} = 1/N$, where Ng is the final gravity during the in-flight condition in the centrifuge test.

In the current study, model geogrid reinforcement was used as soil reinforcement. The scaling requirements for geogrid reinforcement in soil models were reported by Viswanadham and König (2004). To simulate the identical strain conditions between the field and the centrifuge, the tensile load (T_u in force/length) and the stiffness (J_g = T_u/ε_{gu}) should be scaled down by $1/N$. Where ε_{gu} is the ultimate strain of geogrid, which is $(\varepsilon_{gu})_m = (\varepsilon_{gu})_p$. The soil-geogrid interface angle and the percent opening area are required to be maintained identically (i.e., ${\phi_{sg}}_m = {\phi_{sg}}_p$ and $f_m = f_p$) to simulate the equal frictional response at the soil-geogrid interface.

Pseudostatic inertial loading on the GRS wall in the centrifuge experiment was applied using a tilt-table simulator reported by Kumar and Viswanadham (2022). The inertial force applied to the GRS model is calculated as $F_\alpha = K_h W$ where W is the weight of the sliding mass and $K_h = tan\,\alpha$ is the equivalent horizontal seismic coefficient that is achieved by rotating the tilt table by an angle of α. Kumar and Viswanadham (2022) have reported that the pseudostatic seismic load/inertial force $(F_\alpha)_m = (F_\alpha)_p/N^2$ and scaling factor for the rotation angle remains unity, i.e., $\alpha_m = \alpha_p$.

The GRS wall facing was scaled down following the recommendations given by Viswanadham et al. (2017), considering the equivalent flexural rigidity of the facing elements, i.e.,

$$ {t_f}_m/{t_f}_p = \frac{1}{N}\left[\frac{{E_f}_p}{{E_f}_m}\right]^{1/3} \quad (1) $$

Table 1. Properties of sand used as backfill and foundation

Parameter	Backfill soil	Foundation soil
Relative Density (RD)	55%	85%
Unit Weight (kN/m³)	14.71	15.53
Friction Angle	34°	38°

3. MATERIALS

3.1 Soil

The fine sand used in the GRS wall model is sourced Goa state of India and placed at different relative densities (RD) for foundation and backfill. With d_{50}= 0.2 mm, e_{max}= 0.94, e_{min}= 0.63, C_u=2.1 and C_c=1.1, the fine sand (passing through 0.425 mm sieve) was classified as poorly graded fine sand (SP) according to unified soil classification system. Table 1 summarises the engineering and index properties of the sand.

3.2 Geogrid reinforcement

A model geogrid made of polyester-polyvinyl chloride polymers was used as reinforcement in the GRS wall model, with the reinforcement's weakest direction (cross-machine direction (CMD)) aligned with the loading direction. Wide-width tensile tests according to ASTM D4595 (2011) were conducted to obtain the tensile properties of the geogrid. The peak tensile strength and the secant stiffness (J_g) at 2% strain (ϵ_g) of the geogrid model were obtained as 0.93 kN/m (37.2 kN/m in prototype dimension) and 10 kN/m (400 kN/m in prototype dimension), respectively. The properties of the geogrid reinforcement are summarised in Table 2.

Table 2. Properties of model geogrid reinforcement (values within parentheses indicate prototype values)

Parameter	Value
Material	PET+PVC
Thickness at 2 kPa (mm)	0.8
Secant stiffness at 2% strain, J_g (kN/m)	10 (400)
Ultimate tensile load, T_u (kN/m)	0.93 (37.2)
Ultimate tensile strain, ϵ_{gu} (%)	19.4
Soil-geogrid interface friction angle, ϕ_{sg} (°)	29.6

3.3 GRS wall facing

The model wall facing was fabricated in the laboratory using marine plywood to replicate the concrete panels utilised in the field. Three individual sheets of marine plywood were pasted together to form the model facing, having a final thickness of 7.2 mm. Flexural tensile tests as per IS: 1734 (1983) were conducted on the model facings which concluded the elastic modulus of the panel to be 2270 MPa (in model dimension) From the scaling principle of the panel thickness in Eq. (1) the 7.2 mm thick model panel simulates a concrete (M30 grade) prototype panel of 100-120 mm thickness at 40g gravity level.

The internal connection between the concrete panels in the field was simulated using a mortise-and-tenon connection between the facing panels in the model. The geogrid reinforcement was connected to the panel using a 2.2 mm stainless-steel rod passing

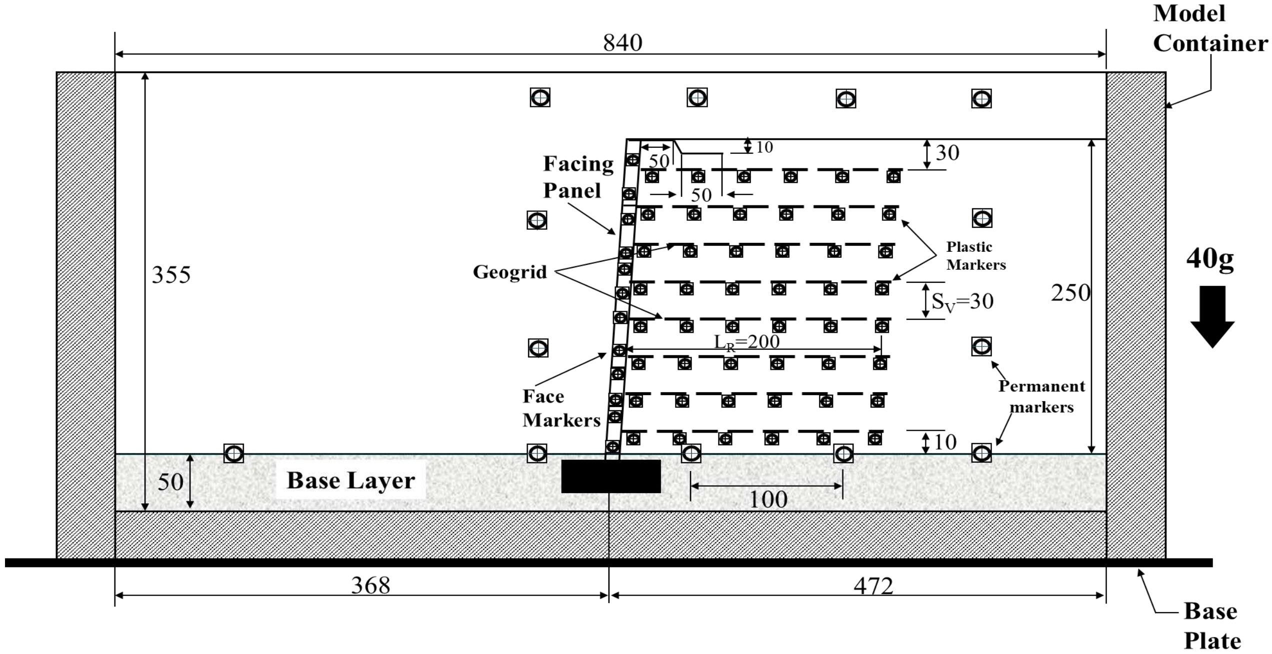

Figure 1. Schematic of GRS wall model (all dimensions are in mm)

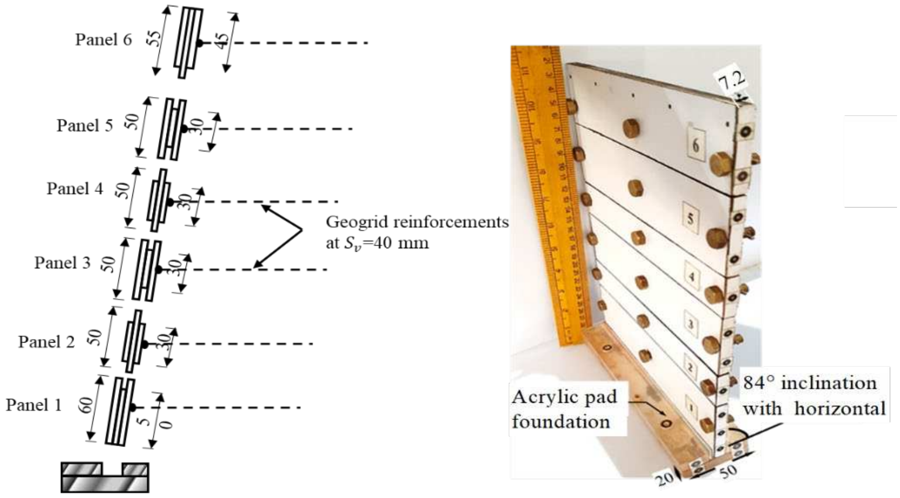

(a)

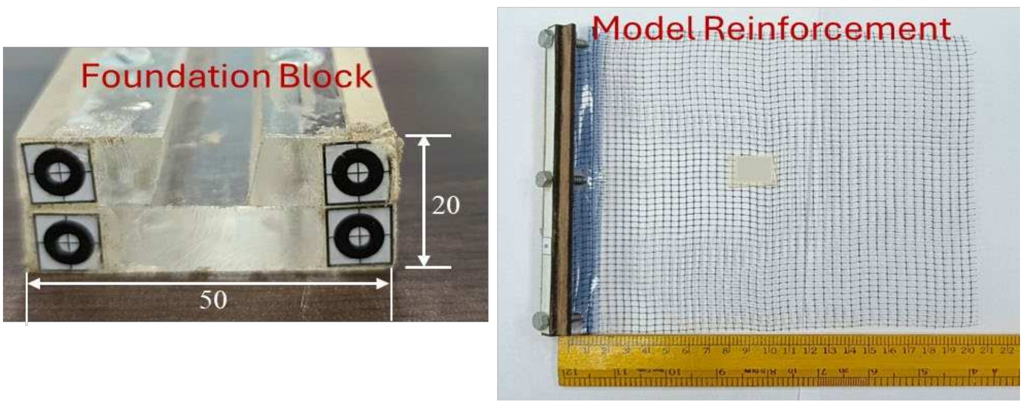

(b)

Figure 2. (a) Panel orientation; (b) Foundation block and reinforcement connected to panel (all dimensions are in mm).

through a loop in the reinforcement and attached to the panel with screws.

4. CENTRIFUGE MODEL PREPARATION

The dimensions mentioned in this section represent the model dimensions unless mentioned otherwise. The experiments were conducted using the large beam geotechnical centrifuge with 4.5 m radius available at the National Geotechnical Centrifuge Facility of the Indian Institute of Technology Bombay, India. The details of the centrifuge facility can be found in Chandrasekharan (2001). The schematic of the GRS wall model tested in the centrifuge at 40g is presented in Figure 1. The GRS wall model was prepared inside the aluminium container having internal dimensions ($L \times B \times H$) 950 mm ×350 mm×250 mm. Plywood formwork was placed inside the aluminium tank to obtain the final internal dimensions of 840 mm × 350 mm × 200 mm. The front of the container is made of a 20 mm thick Perspex sheet. Thin plastic sheets were

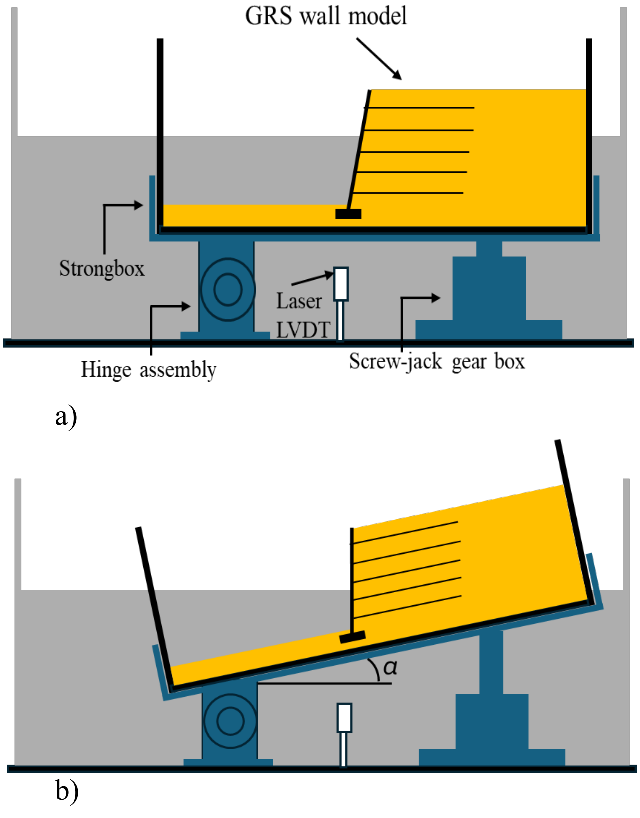

Figure 3. Schematic of GRS model mounted on tilt-table; a) At $\alpha = 0°$ and b) At the onset of inducing tilt

placed on the front Perspex sheet and the rear wall to reduce boundary effects at the soil-container interface. The GRS wall model consists of 6 layers of geogrid reinforcement, each 200 mm long, spaced vertically at 40 mm. Figure 2 shows different components of the facing panels and the foundation block.

The GRS wall model was constructed with sand as backfill material, with a wall height of 250 mm on a foundation layer of 50 mm thickness. The air pluviation technique was used to prepare the GRS wall model with dry sand. A laboratory-fabricated sand-raining device was employed for pluviation, calibrated to achieve the desired RD of the compacted sand. The foundation was constructed with an RD of 85% and the backfill had a comparatively lower RD of 55% to simulate poor compaction conditions.

The model preparation started with placing the foundation layer to a height of 25 mm. At this stage, a 50 mm wide and 20 mm thick acrylic foundation block (see Figure 2b) was placed, with a slanted groove to maintain the desired 84° batter angle of the wall. The first panel was then placed on the foundation block, and additional props were added to maintain its position during model preparation. Thereafter, soil filling continued for the remainder of the foundation layer. Upon completion of the foundation layer, sand was placed in the first backfill layer up to the height of the first geogrid layer. Upon completion of the first backfill layer, the reinforcement was laid on the sand, followed by the installation of the next panel. Subsequently, the additional layers were placed, and the props were removed to complete the other half of the foundation layer at the front of the wall. The compacted density of the sand was continuously checked during the model construction by placing a small aluminium can in the container and measuring the density of the sand accumulated inside it. Very similar to field conditions, a nonwoven geotextile layer measuring 200 mm in length was wrapped within the backfill, as shown in Figure 1. Small plastic markers with crosshairs were pasted on the geogrid layers and the facing panels to obtain wall and reinforcement deformation readings.

4. PSEUDOSTATIC LOAD SIMULATOR

The pseudostatic inertia force was simulated using an in-house-developed tilt-table-based simulator. This simulator consists of a C-section mounted on a hinge assembly on one side and a screw jack system on the other. The model container is placed on the C-section as shown in Figure 3. The pseudostatic load simulator is controlled during in-flight conditions to rotate the C-section plate at speeds ranging from 0.2°/min to 0.8°/min. The simulator can be rotated, as shown in Figure 4, up to a maximum angle of 20°, producing K_h= Tan 20° = 0.36. Further features and merits of this tilt table simulator are discussed in Kumar and Viswanadham (2022).

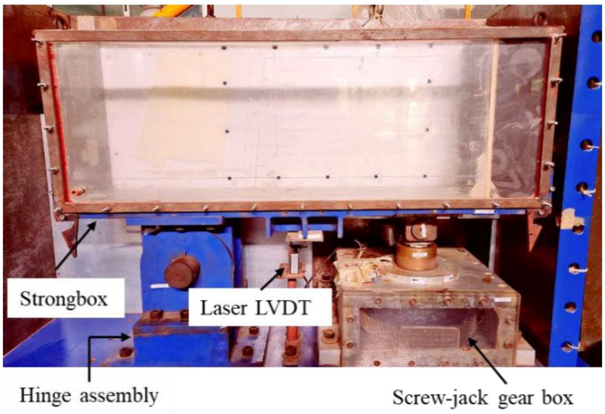

Figure 4. Model container and tit-table arrangements.

5. METHODS OF IMAGE ANALYSIS

The strain and deformation in the soil and reinforcements were obtained using advanced image analysis methods, including digital image analysis (DIA) and particle image velocimetry (PIV). A GoPro digital camera was placed in front of the perspex wall to capture continuous images during the experiment at 5 s intervals from the onset of centrifuge operation. These images were further processed in the open-source programme ImageJ to obtain the displacement of the plastic markers pasted on the reinforcements and the facing panels, followed by the calculation of reinforcement strains and wall-facing deformations.

For the PIV analysis, 1 mm fine glass beads were smeared onto the inner surface of the Perspex wall using a thin layer of transparent grease to ensure proper adhesion and image contrast. The open-source MATLAB code GeoPIV (Stanier et al., 2015) was used to process the images and obtain soil deformation contours.

6. RESULTS

The following sections present the results from the DIA analysis on GRS wall-facing deformations and reinforcement strains, followed by the soil deformation contours from the PIV analysis.

6.1 Wall deformation

The wall facing deformations are plotted in Figure 5. The results in Figure 5(a) indicate that wall-facing deformation increased with increasing seismic load intensity. The maximum facing deformation was observed at a height of 0.65H, whereas there was negligible deformation at the base. This indicates a bulging failure caused by lateral earth pressure and seismic thrust. It is noted that the maximum wall deformation exceeded the allowable displacement of 4% (FHWA, 2009) at K_h=0.16 and reached a peak value of 8.5% at the penultimate stage of K_h=0.27. The amplification factors, defined as the ratio of the maximum facing deformation due to the seismic loading to the deformation under the static case ($\delta_{dyn}/\delta_{stat}$) are plotted in Figure 5(b). The results indicate that amplification in the facing displacements increases with wall height, reaching a maximum at the top. For example, the amplification factor at the base, i.e., z=0.078H, is 2.5. At the same time, the wall deformation is amplified by 8 times at the top of the wall, i.e., z=0.98H. This significant increase in the facing displacements can be attributed to the additional active thrust exerted on the wall due to the pseudostatic seismic load. These excessive deformations necessitate greater attention to the serviceability criteria of GRS walls during their design in seismically active zones.

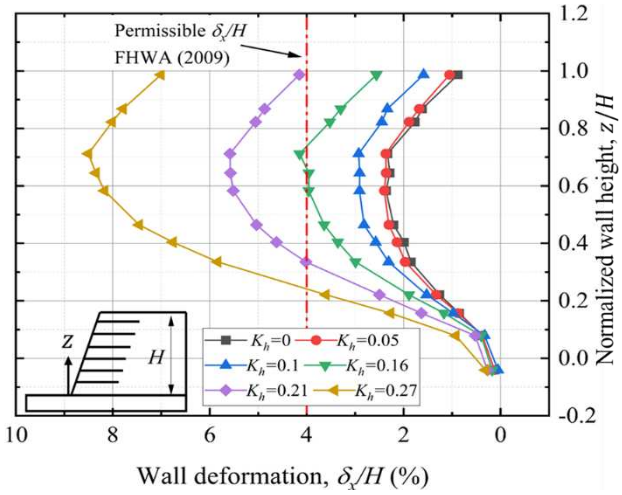

(a)

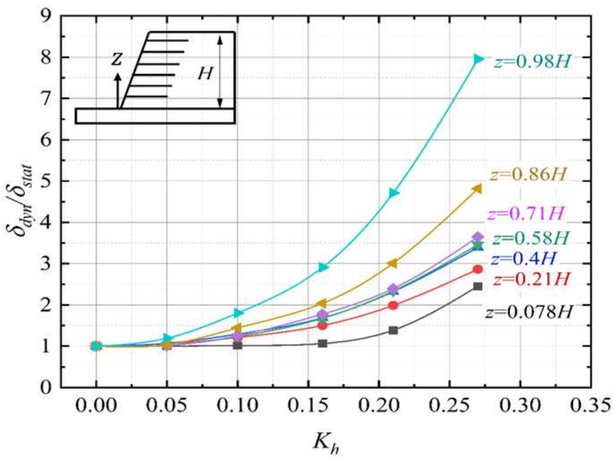

(b)

Figure 5. (a) Variation in wall facing displacement with seismic loading; (b) amplification in the wall facing displacement.

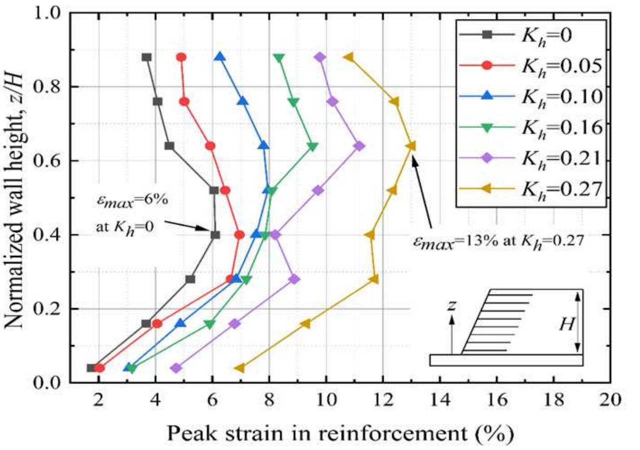

Figure 6. Variation in peak reinforcement strain along the wall height.

6.2 Reinforcement strains

The reinforcement strains obtained from the DIA analysis are plotted in Figure 6. The strains were computed using the following expression (Viswanadham and Mahajan, 2007):

$$\varepsilon(\%) = \left(\sqrt{\frac{(x_2^f - x_1^f)^2 + (y_2^f - y_1^f)^2}{(x_2^i - x_1^i)^2 + (y_2^i - y_1^i)^2}} - 1 \right) \times 100 \qquad (2)$$

The results plotted in Figure 6 indicate a similar amplification of the reinforcement strains with increasing seismic load intensity. The maximum reinforcement strain increased from 6% at the static condition (K_h=0) to 13% at the penultimate stage (K_h=0.27). This increase in reinforcement strain under seismic conditions is caused by tensile forces induced by the active thrust generated by seismic loading. It is noted that the maximum reinforcement strains are observed at the location of maximum wall facing displacements.

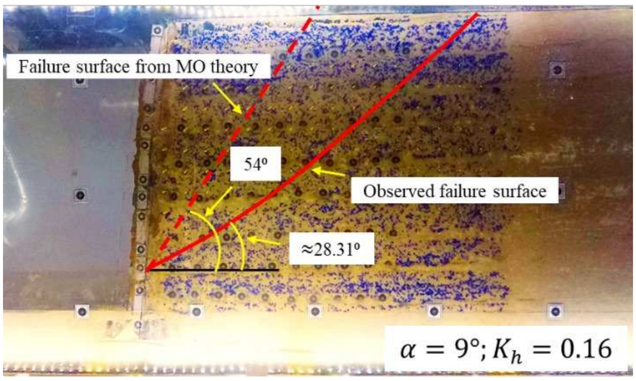

(a)

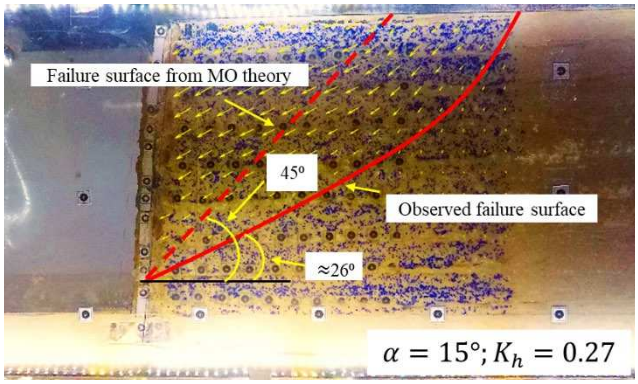

(b)

Figure 7. Inclination of active failure wedge observed under seismic loading for (a) $\alpha = 9°; K_h = 0.16$; (b) $\alpha = 15°; K_h = 0.27$.

6.3 Soil deformation and failure wedge

The soil displacement contours were obtained from PIV analysis and are plotted in Figures 7 and 8 for two particular K_h values. Figure 7 shows the failure wedge inclination, which evolves with a change in the seismic load intensity. A curved failure wedge was observed within the soil mass. The inclination of the wedge reduced from 28.31° at K_h=0.16 to 26° at K_h=0.27. This reduction in the inclination angle indicates a widening of the active wedge and higher active thrust on the wall, resulting in higher wall-facing displacements and reinforcement strains, as observed in Figures 5 and 6. It should be noted that the analytical Mononobe-Okabe theory (Batrhurst and Cai, 1995) significantly underestimates the wedge inclination as indicated in Figure 7. This underestimation can lead to an underconservative or unsafe design of the GRS wall, as the location of the failure plane affects the anchored length of the reinforcement extending beyond it. This anchored length primarily contributes to the stability of the GRS wall by mobilising tensile forces and resisting lateral thrust. The soil displacement contours plotted in Figure 8 support the widening of the failure wedge through rotation of the active failure plane.

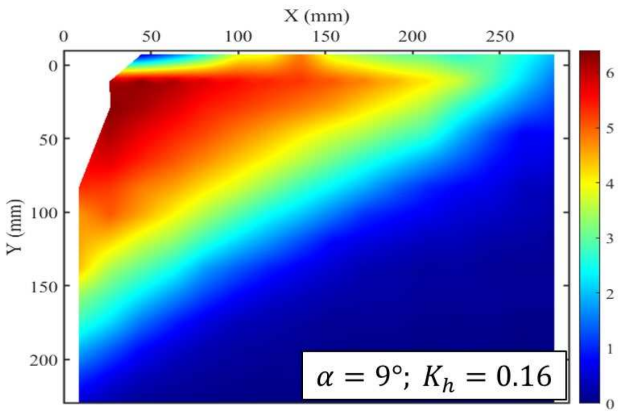

(a)

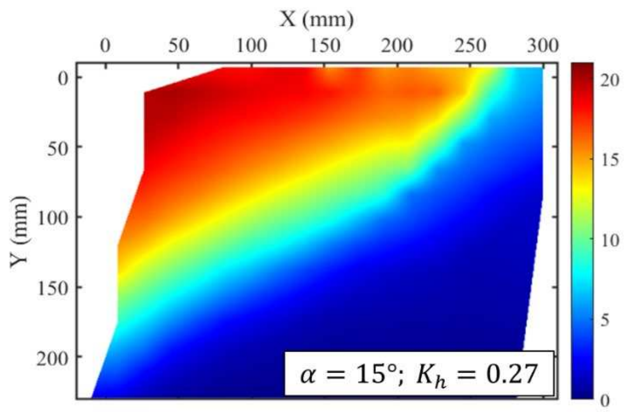

(b)

Figure 8. Soil deformation contours obtained from PIV analysis (a) $\alpha = 9°; K_h = 0.16$*; (b)* $\alpha = 15°; K_h = 0.27$.

6. CONCLUSIONS

This paper presents the results of a centrifuge test on the GRS wall under pseudostatic seismic conditions. The results from the DIA and PIV analyses are presented to indicate wall-facing displacements, reinforcement strains, and soil deformation. The following conclusions can be drawn from the findings:

- The GRS wall facing displacements increased significantly with an increase in the seismic load intensity. The permissible wall displacement of 4% was exceeded at an acceleration of 0.16*g*.
- Similar to the facing displacement, the reinforcement strains are amplified with an increase in the pseudostatic acceleration. The maximum reinforcement strain was observed at a height of 2/3H, which also coincided with the location of the maximum wall facing displacement.
- The active failure plane rotated due to the expansion of the failure wedge with an increase in the K_h value. The theoretical Mononobe-Okabe theory is found to underestimate the failure plane inclination, potentially leading to an unsafe design of GRS walls under seismic conditions.

In conclusion, the observed increase in wall-facing deformations, together with the amplified strains in the reinforcements, underscores the need for greater emphasis on serviceability limits when designing GRS walls under seismic loading. Excessive facing deformation can endanger nearby structures, while the persistence of high tensile strains in polymeric reinforcements may induce creep, reduce their load-carrying capacity, and potentially trigger progressive deformation or even structural failure of the wall.

ACKNOWLEDGEMENTS

The authors are grateful for the financial support received by the first author from the Indian Institute of Technology Bombay, India, under the institute's postdoctoral fellowship, and from the Department of Science and Technology (DST) under the INSPIRE faculty fellowship.

REFERENCES

ASTM (2011). *Standard test method for tensile properties of geotextiles by the wide-width strip method*. ASTM D4595. West Conshohocken, PA.

Bathurst, R. J. & Cai, Z. (1995). Pseudo-static seismic analysis of geosynthetic-reinforced segmental retaining walls. *Geosynthetics International*, 2(5): 787–830. https://doi.org/10.1680/gein.2.0037

BIS (Bureau of Indian Standards) (1983). *Methods of test for plywood*. IS:1734. New Delhi, India.

Chandrasekaran, V. S. (2001). Numerical and centrifuge modelling in soil structure interaction. *Indian Geotech. J*. 31 (1): 30–59.

El-Emam, M. M. & Bathurst, R. J. (2007). Influence of reinforcement parameters on the seismic response of reduced-scale reinforced soil retaining walls. *Geotextiles and Geomembranes*, 25(1): 33–49. https://doi.org/10.1016/j.geotexmem.2006.09.001

Kumar, P., Viswanadham, B.V.S., (2022). Design and Development of Tilt Table-Based Inflight Simulator for Pseudostatic Loading in a Geotechnical Centrifuge. *Geotech. Test J*., ASTM 45(5): 936–960. https://doi.org/10.1520/GTJ20210216

Latha, G.M. & Santhanakumar, P. (2015). Seismic response of reduced-scale modular block and rigid faced reinforced walls through shaking table tests. *Geotextiles and Geomembranes*, 43(4): 307–316. https://doi.org/10.1016/j.geotexmem.2015.04.008

Stanier, S.A., Blaber, J., Take, W.A. and White, D.J. (2015). Improved image-based deformation measurement for geotechnical applications. *Canadian Geotechnical Journal* 53(5): 727-739. https://doi.org/10.1139/cgj-2015-0253

Viswanadham, B. V. S., and D. König. (2004). Studies on scaling and instrumentation of a Geogrid. *Geotext. Geomembr.* 22 (5): 307–328. https://doi.org/10.1016/S0266-1144(03)00045-1

Viswanadham, B. V. S., H. R. Razeghi, J. Mamaghanian, and C. H. S. G. Manikumar. (2017). Centrifuge model study on geogrid reinforced soil walls with marginal backfills with and without chimney sand drain. *Geotext. Geomembr*. 45(5): 430–446. https://doi.org/10.1016/j.geotexmem.2017.06.005

Viswanadham, B.V.S., Mahajan, R.R. (2007). Centrifuge model tests on geotextilereinforced slopes. *Geosynth. Int*. 14 (6): 365–379. https://doi.org/10.1680/gein.2007.14.6.365